HHS Public Access

Author manuscript

Gut. Author manuscript; available in PMC 2021 October 01.

Published in final edited form as:

Gut. 2021 October ; 70(10): 1933–1945. doi:10.1136/gutjnl-2020-321548.

ATF4 activation promotes hepatic mitochondrial dysfunction by repressing NRF1-TFAM signaling in alcoholic steatohepatitis.

Liuyi Hao[1], **Wei Zhong**[1,2], **Haibo Dong**[1], **Wei Guo**[1], **Xinguo Sun**[1], **Wenliang Zhang**[1], **Ruichao Yue**[1], **Tianjiao Li**[1], **Alexandra Griffiths**[4], **Ali Reza Ahmadi**[3], **Zhaoli Sun**[3], **Zhenyuan Song**[4], **Zhanxiang Zhou**[1,2,*]

[1]Center for Translational Biomedical Research, University of North Carolina at Greensboro, North Carolina Research Campus, Kannapolis, NC, USA.

[2]Department of Nutrition, the University of North Carolina at Greensboro, North Carolina Research Campus, Kannapolis, NC, USA.

[3]Department of Surgery, Johns Hopkins University School of Medicine, Baltimore, Maryland, USA.

[4]Department of Kinesiology and Nutrition, College of Applied Health Sciences, the University of Illinois at Chicago, Chicago, IL, USA.

Abstract

Objective: Mitochondrial dysfunction plays a dominant role in the pathogenesis of alcoholic liver disease (ALD); however, the underlying mechanisms remain to be fully understood. Activating transcription factor 4 (ATF4) regulates genes involved in steatosis, oxidative stress, and apoptosis. This study aimed to investigate the function and mechanism of ATF4 in alcohol-induced hepatic mitochondrial dysfunction.

Design: ATF4 activation was detected in the livers of patients with alcoholic hepatitis (AH). The role of ATF4 and mitochondrial transcription factor A (TFAM) in alcohol-induced liver damage was determined in hepatocyte-specific *ATF4* knockout mice and liver-specific *TFAM* overexpression mice, respectively.

Results: Hepatic PERK-eIF2α-ATF4 ER stress signaling was upregulated in the livers of patients with AH. Hepatocyte-specific ablation of *ATF4* in mice ameliorated alcohol-induced hepatic steatosis, inflammation, and cell death. *ATF4* ablation attenuated alcohol-impaired mitochondrial biogenesis and respiratory function along with the restoration of TFAM. Cell studies confirmed that TFAM expression was negatively regulated by ATF4. *TFAM* silencing in hepatoma cells abrogated the protective effects of *ATF4* knockdown on ethanol-mediated

[*]**Corresponding author:** Zhanxiang Zhou, Center for Translational Biomedical Research and Department of Nutrition, the University of North Carolina at Greensboro, North Carolina Research Campus, 600 Laureate Way, Suite 2203, Kannapolis, NC 28081. Phone: 704-250-5800 Fax: 704-250-5809 z_zhou@uncg.edu.

Author Contributions: L.H. and Z.Z conceived and designed research; L.H., H.D., X.S., W.G, W.Z., W.L.Z, R.Y., T.L., and Z.Z. performed experiments and data analysis. A.A. and Z.S. collected human samples and acquired clinical data. All the authors participated in manuscript preparation.

Conflicts of Interest: No potential conflicts of interest relevant to this article are reported.

Patient consent: Obtained.

mitochondrial dysfunction and cell death. Moreover, hepatocyte *TFAM* overexpression in mice attenuated alcohol-induced mitochondrial dysfunction and liver damage. Mechanistic studies revealed that ATF4 repressed the transcription activity of *NRF1*, a key regulator of TFAM, through binding to its promoter region. Clinical relevance among ATF4 activation, NRF1-TFAM pathway disruption, and mitochondrial dysfunction was validated in the livers of patients with AH.

Conclusion: This study demonstrates that hepatic ATF4 plays a pathological role in alcohol-induced mitochondrial dysfunction and liver injury by disrupting the NRF1-TFAM pathway.

Keywords

Alcoholic liver disease; ER stress; mitochondrial biogenesis; OXPHOS

Introduction

Alcoholic liver disease (ALD), caused by long-term excessive alcohol consumption, represents one of the most prevalent types of chronic liver diseases worldwide [1, 2]. ALD encompasses a broad spectrum of clinical features ranging from simple fatty liver to more advanced steatohepatitis, fibrosis, cirrhosis, and, ultimately, hepatocellular carcinoma [3]. Hepatocyte is densely packed with mitochondria, which is the principal site of adenosine triphosphate (ATP) generation. Mitochondria integrate cell metabolism by regulating essential anabolic and catabolic pathways that ultimately depends on the proper function of oxidative phosphorylation (OXPHOS) [4, 5]. The OXPHOS system consists of 5 multisubunit complexes that are encoded by both nuclear DNA and mitochondrial DNA (mtDNA). The correct balance among mitochondrial complexes is essential to maintain cellular homeostasis and linked to cell fate decision [6, 7]. During the initiation and progression of ALD, hepatic mtDNA deletion/mutation and decreased respiratory chain complexes activities are intimately associated with liver damage in both human and mice [8–10].

Alcohol consumption induces accumulation of unfolded or misfolded proteins in the Endoplasmic reticulum (ER) lumen, which activates unfolded protein response (UPR) via the induction of protein kinase RNA-like endoplasmic reticulum kinase (PERK) [11]. As a result, the level of phosphorylated eukaryotic initiation factor 2 alpha (eIF2α) is distinctly elevated, resulting in the nuclear translation of activating transcription factor 4 (ATF4) [12]. ATF4 is a member of the cAMP-responsive element-binding protein family of basic zipper-containing proteins, regulates a variety of genes involved in various physiological processes, including apoptosis, lipid metabolism, and obesity [13–17]. Loss of *ATF4* in HeLa cells led to enhanced ATP-dependent respiration, suggesting that ATF4 regulates mitochondrial functions [18]. Our previous studies have shown that alcohol-induced hepatic mitochondrial dysfunction was associated with ATF4 activation [19]. However, whether ATF4 regulates mitochondrial functions in the liver remains unclear. Considering ER stress is a pathological factor for mitochondrial dysfunction in multiple cell lines [20–22], and ATF4 activation plays a detrimental role in alcoholic steatosis [16], we hypothesized that ATF4 might be involved in the pathogenesis of alcohol-induced hepatic mitochondrial dysfunction.

Materials and Methods

Materials and methods used in this study were described in Supplementary Materials and Methods.

Results:

The hepatic PERK-eIF2α-ATF4 ER stress signaling pathway is upregulated in patients with alcoholic hepatitis.

Compared with healthy subjects, alcoholic hepatitis (AH) patients exhibited robustly enhanced phosphorylation of PERK and eIF2α proteins in the liver (Fig. 1A). The total protein levels of hepatic PERK and eIF2α were comparable between two groups (Supplementary Fig. 1A). Hepatic protein levels of ATF4 were markedly increased by 9-fold in AH patients, as evaluated by Western blot (Fig. 1A). Increased hepatic protein expression of ATF4 was also detected by IHC staining (Fig. 1A). In contrast to the cytoplasmic localization of PERK and eIF2α, ATF4 was primarily localized in the nuclei of hepatocytes (Fig. 1A). Hepatic mRNA levels of ATF4 were also upregulated by 5-fold in AH patients (Fig. 1B).

Hepatocyte-specific deletion of *ATF4* alleviates alcohol-induced liver injury.

To determine the role of ATF4 in the pathogenesis of ALD, hepatocyte-specific *ATF4* knockout ($ATF4^{\Delta Hep}$) mice were generated (Supplementary Fig. 1B). ATF4 floxed mice and $ATF4^{\Delta Hep}$ mice were subjected to the Lieber-DeCarli control diet (Flox/PF or $ATF4^{\Delta Hep}$/PF) or alcohol diet (Flox/AF or $ATF4^{\Delta Hep}$/AF) for eight weeks plus a single binge (4 g/kg) before four hours of tissue collection (modified NIAAA model). Chronic alcohol feeding activated the PERK-eIF2α-ATF4 signaling pathway in the liver of floxed mice (Fig. 1C and Supplementary Fig. 1B). Only trace amounts of ATF4 proteins were detected in the livers of $ATF4^{\Delta Hep}$/AF mice despite the PERK-eIF2α signaling activation (Fig. 1C and Supplementary Fig. 1C). As shown in Fig. 1D, liver histopathological changes induced by chronic alcohol feeding, including lipid droplet accumulation and inflammatory cell infiltration, were alleviated in $ATF4^{\Delta Hep}$ mice. Alcohol-increased hepatic triglyceride (TG) and free fatty acid (FFA) contents were attenuated by *ATF4* deletion (Supplementary Fig. 2A and B). The liver weight and body weight were comparable among all groups (Supplementary Fig. 2C). Alcohol-increased serum levels of alanine aminotransferase (ALT) and aspartate aminotransferase (AST) were also ameliorated by *ATF4* deletion (Fig. 1E).

Neutrophils infiltration in the liver was analyzed by flow cytometry with a gating strategy showed in Supplementary Fig. 3A. Chronic alcohol feeding increased the frequency of neutrophils ($CD45^+CD11b^+Ly6g^+$) in the livers of floxed mice, and this effect was ameliorated by *ATF4* deletion (Fig. 1F). Correspondingly, $ATF4^{\Delta Hep}$/AF mice displayed fewer hepatic myeloperoxidase (MPO) positive cells than Flox/AF mice (Supplementary Fig. 3B). Both the protein and mRNA levels of hepatic chemokine (C-X-C motif) ligand 1 (CXCL-1) were increased after alcohol exposure, whereas these effects were reversed by *ATF4* ablation (Supplementary Fig. 3C). However, alcohol-increased number of hepatic

F4/80 positive cells and abundance of $CD45^{\pm}CD11b^{int}F4/80^{hi}$ macrophage were not significantly affected by *ATF4* ablation (Supplementary Fig. 3D and E).

In response to alcohol feeding, TUNEL positive cells were both detected in the livers of floxed mice and $ATF4^{\Delta Hep}$ mice compared with their corresponding controls; with *ATF4* deletion, mice displayed fewer positive cells (Fig. 1G). Alcohol-increased hepatic protein levels of B-cell lymphoma 2 (Bcl-2), p53 upregulated modulator of apoptosis (PUMA), and cleaved caspase-3 (cCASP3) were all ameliorated in $ATF4^{\Delta Hep}$ mice (Fig. 1G). However, alcohol-induced hepatic C/EBP homologous protein (CHOP) activation was not affected by *ATF4* deletion (Fig. 1G). Hepatic protein levels of alcohol metabolizing enzymes, including alcohol dehydrogenases (ADH) and cytochrome P450 2E1 (CYP2E1), and serum ethanol levels were comparable in Flox/AF mice and $ATF4^{\Delta Hep}$/AF mice (Supplementary Fig. 4A and B).

Hepatocyte-specific deletion of *ATF4* protects alcohol-induced mitochondrial dysfunction in mice.

We further determined if *ATF4* deletion can improve alcohol-induced mitochondrial dysfunction. Primary hepatocytes from $ATF4^{\Delta Hep}$ mice displayed a markedly higher mitochondrial respiration than those from floxed mice fed with either control or alcohol diet (Fig. 2A). Alcohol-decreased basal oxygen consumption rate (OCR) was almost completely normalized by *ATF4* knockout (Fig. 2A). We examined the effects of ATF4 and alcohol on mitochondrial fatty acid β-oxidation (FAO) in primary hepatocytes. Primary hepatocytes were incubated with fatty acids before flux analysis. In this condition, hepatocytes from $ATF4^{\Delta Hep}$ mice showed enhanced OXPHOS compared with those from floxed mice (Fig. 2A). Alcohol-decreased FAO was also largely preserved by hepatic *ATF4* deletion (Fig. 2A). $ATF4^{\Delta Hep}$/AF mice displayed significantly higher levels of hepatic ATP contents compared with Flox/AF mice (Fig. 2B).

We next measured the levels of mitochondrial reactive oxygen species (mtROS) and total ROS in primary hepatocytes. Compared with Flox/PF mice, higher mtROS and total ROS levels were detected in the hepatocytes from Flox/AF mice, whereas these effects were ameliorated by hepatic *ATF4* knockout (Fig. 2C and Supplementary Fig. 5A). Alcohol-increased 4-hydroxynonenal (4-HNE) protein adducts formation in the liver was attenuated in $ATF4^{\Delta Hep}$ mice (Supplementary Fig. 5B). Hepatocytes isolated from Flox/AF mice exhibited significantly lower mitochondrial membrane potential than those from Flox/PF mice, whereas this effect was ameliorated in $ATF4^{\Delta Hep}$ mice (Fig. 2D). The enzymatic activity of mitochondria respiratory complex I, which control cellular NAD^+/NADH redox balance, was decreased by chronic alcohol feeding in floxed mice (Fig. 2E). *ATF4* deletion not only restored alcohol-reduced mitochondria respiratory complex I activity (Fig. 2E), but also corrected alcohol-decreased NAD^+ contents and NAD^+/NADH ratio in the liver (Supplementary Fig. 5C).

We next analyzed the effects of alcohol and ATF4 on hepatic mitochondrial respiratory chain (MRC) complexes, the proper function of which are essential for maintaining mitochondrial homeostasis. The protein levels of mtDNA-encoded mitochondrial complexes subunits, including cytochrome c oxidase subunit 1 (MTCO1) (Fig. 2F and G) and mitochondrial

encoded ATP synthase membrane subunit 6 (MTATP6) (Fig. 2G), were remarkably higher in ATF4$^{\Delta Hep}$ mice than that in floxed mice, regardless of alcohol administration. Alcohol-decreased protein levels of nuclear genome-encoded complexes were also reversed by *ATF4* knockout (Fig. 2G). Furthermore, hepatic relative mtDNA contents (*MTND1* relative to *SDHA*) and mRNA levels of mtDNA-encoded complexes subunits were all significantly increased in ATF4$^{\Delta Hep}$ mice on either diet compared with floxed mice (Fig. 2H and Supplementary Fig. 6A and B). After chronic alcohol exposure, mitochondria in hepatocyte appear swollen with few cristae, whereas these changes were reversed by hepatic *ATF4* knockout (Fig. 2I).

ATF4 negatively regulates TFAM expression in hepatocyte.

To understand the mechanisms underlying *ATF4* deletion-restored hepatic mtDNA contents in ALD, major regulators involved in mtDNA replication, transcription, and maintenance were examined. Intriguingly, ATF4$^{\Delta Hep}$ mice displayed higher hepatic TFAM mRNA and protein levels on either diet compared with their genetic controls, as evaluated by RT-PCR (Fig. 3A), Western blot (Fig. 3B), and IHC staining (Fig. 3C). However, the mRNA levels of DNA polymerase subunit gamma (Plog), DNA-directed RNA polymerase, mitochondrial (Polrmt), and twinkle mtDNA helicase (Twinkle) were comparable between Flox/AF mice and ATF4$^{\Delta Hep}$/AF mice (Fig. 3A). Furthermore, the association between ATF4 induction and TFAM reduction was observed in the liver from mice fed with ethanol for four weeks (Supplementary Fig. 7A).

To verify the animal data *in vitro*, we used VL-17A cells, a recombinant HepG2 cell line that constitutively expresses human ADH and CYP2E1 for efficient alcohol metabolism. Alcohol administration enhanced the expression of PERK-eIF2α-ATF4 signaling but decreased the expression of TFAM in a time- and dose-dependent manner in VL-17A cells (Supplementary Fig. 7B and C). We next created the stable *ATF4* overexpression and knockdown cell lines, respectively, by using the CRISPR-Cas9 approach. The efficiency of *ATF4* overexpression and knockdown in VL-17A cells was confirmed by Western blot (Fig. 3D) and RT-PCR (Fig. 3E). Both the protein and mRNA levels of TFAM were downregulated by *ATF4* overexpression, while upregulated by *ATF4* knockdown (Fig. 3D and E). Correlative to the changes in TFAM, the mtDNA contents (Fig. 3F), *MTCO1* mRNA levels (Fig. 3G), and protein levels of the mtDNA-encoded genes, including Cytochrome b (MTCYB), MTCO1, and MTATP6, (Fig. 3G, H) were all markedly decreased by *ATF4* overexpression but increased by *ATF4* knockdown in VL-17A cells compared with the control cells.

TFAM reduction is involved in ATF4-mediated mitochondrial dysfunction in VL-17A cells with alcohol exposure.

To further determine whether TFAM is the key molecule mediating the effect of ATF4 on mitochondrial function under alcohol exposure, *TFAM* knockdown, and *ATF4/TFAM* double knockdown VL-17A cell lines were established and were treated with alcohol. As shown in Fig. 4A, cellular protein levels of ATF4 and TFAM were dramatically reduced by gene knockdown. *ATF4* knockdown-increased protein levels of TFAM were entirely abrogated by *TFAM* knockdown in VL-17A cells (Fig. 4A). *TFAM* knockdown

led to a severe reduction of mtDNA levels and exacerbated alcohol-decreased mtDNA levels in VL-17A cells (Fig. 4B). Moreover, the protective role of *ATF4* knockdown in alcohol-mediated mtDNA depletion was completely abolished by *TFAM* knockdown (Fig. 4B). The same trend was also observed in the mRNA levels of *MTCO1* in VL-17A cells (Supplementary Fig. 8A). Alcohol-decreased mitochondrial complex I activity was also ameliorated by *ATF4* knockdown but exacerbated by *TFAM* knockdown (Supplementary Fig. 8B). *ATF4* knockdown cells exhibited a higher respiration rate and attenuated ethanol-decreased basal OCR, whereas these effects were abrogated by *TFAM* knockdown (Fig. 4C). Although *TFAM* knockdown and ethanol exposure did not affect the ATP contents in VL-17A cells, reduction in ATP levels was observed when these two factors combined (Fig. 4D). *ATF4* knockdown protected alcohol-perturbed mitochondrial membrane potential (Fig. 4E). Conversely, *TFAM* knockdown exacerbated the detrimental role of alcohol exposure in mitochondrial membrane potential disruption (Fig. 4E). As shown in Fig. 4F, alcohol exposure significantly increased the protein levels of PUMA and cCASP3, which were ameliorated by *ATF4* knockdown but exacerbated by *TFAM* knockdown (Bar graph shown in Supplementary Fig. 8C). The frequency of Annexin V-positive cells was markedly elevated after alcohol exposure, which was protected by *ATF4* knockdown but aggravated by *TFAM* knockdown (Fig. 4F). Moreover, the protective effects of *ATF4* knockdown on alcohol-induced mitochondrial complex I activity reduction, mitochondrial membrane potential disruption, and apoptotic cell death were all abrogated by *TFAM* knockdown in VL-17A cells (Supplementary Fig. 8B and C and Fig. 4E, F).

TFAM-overexpressing VL-17A cells were generated and subjected to alcohol. Alcohol-decreased TFAM protein levels were completely reversed by *TFAM* overexpression (Fig. 4G). Interestingly, alcohol-induced ATF4 activation was also reversed by *TFAM* overexpression (Fig. 4G). *TFAM* overexpression increased the cellular mtDNA levels and the mRNA levels of mtDNA-encoded complexes subunits regardless of alcohol exposure (Fig. 4H and Supplementary Fig. 9A). However, the mRNA levels of nuclear genome-encoded complexes subunits remain unchanged (Supplementary Fig. 9A). Alcohol-perturbed mitochondrial membrane potential was ameliorated by *TFAM* overexpression in VL-17A cells (Supplementary Fig. 9B). *TFAM* overexpression also reversed alcohol-increased frequencies of Annexin V-positive cells (Fig. 4I). This effect was accompanied by decreased protein levels of PUMA and cleaved caspase-3 (Supplementary Fig. 9C).

Hepatocyte-specific *TFAM* overexpression prevents alcohol-induced mitochondrial dysfunction in mice.

To further validate the protective function of TFAM in alcohol-induced hepatic mitochondrial dysfunction *in vivo*, hepatocyte-specific *TFAM* overexpressing (AAV8-*TFAM*) mice as well as control mice (AAV8-null) were generated. The mRNA and protein levels of TFAM in the liver of *TFAM* overexpressing mice were increased nearly 6-fold and 7-fold, respectively, at the time of starting alcohol feeding (Supplemental Fig. 10A and B). After eight weeks of alcohol feeding, hepatic TFAM protein levels in the AAV8-*TFAM*/AF mice were 5-fold higher than the AAV8-null/AF mice (Fig. 5A). Hepatic mtDNA contents and the mRNA levels of mtDNA-encoded mitochondrial complexes subunits were remarkably increased by *TFAM* overexpression (Fig. 5B). Accordingly, hepatic protein

levels of mtDNA-encoded subunits were higher in AAV8-*TFAM*/AF mice than that in AAV8-null/AF mice (Fig. 5A and Supplemental Fig. 11A). The overexpression of *TFAM* did not affect the expression of nuclear DNA-encoded complexes subunits (Fig. 5A, 5B, and Supplemental Fig. 11A). Overexpression of *TFAM* ameliorated alcohol-impaired mitochondrial respiratory complex I activity (Fig. 5C) along with elevated NAD^+ levels and NAD^+ to NADH ratio in the liver (Supplementary Fig. 11B). Subsequent flow cytometry analysis showed that AAV8-*TFAM*/AF mice displayed higher levels of mitochondrial membrane potential (Fig. 5D) and lower levels of mtROS and total ROS levels in the liver than that in AAV8-null/AF mice (Fig. 5G). Alcohol-decreased hepatic ATP contents were reversed by *TFAM* overexpression (Fig. 5E). Primary hepatocytes from AF/AAV8-*TFAM* mice also displayed higher OCR values in response to either glucose or palmitate (Fig. 5F). Furthermore, alcohol-altered mitochondrial morphology, including swollen and loss of cristae, were reversed by *TFAM* overexpression (Fig. 5H).

Hepatocyte-specific *TFAM* overexpression attenuates alcoholic steatohepatitis.

We found that AAV8-*TFAM*/AF mice displayed markedly fewer hepatic lipid droplets and infiltrated immune cells in the liver compared with AAV8-null/AF mice (Fig. 6A). Lower levels of serum ALT and AST were observed in AAV8-*TFAM*/AF mice than that in AAV8-null/AF mice (Fig. 6B). *TFAM* overexpression in the hepatocytes also decreased neutral lipid accumulation and TG and FFA contents in the liver under alcohol exposure condition (Fig. 6C).

TFAM overexpression ameliorated alcohol-mediated neutrophils infiltration in the liver (Fig. 6D and Supplementary Fig.12A). The mRNA levels of hepatic *CXCL1* and *Ly6g* were also lower in AAV8-*TFAM*/AF (Fig. 6E). However, the number of F4/80 positive cells were not significant affected by *TFAM* overexpression (Supplementary Fig.12B). The number of TUNEL positive cells was reduced in the liver of AAV8-*TFAM*/AF mice (Fig. 6F). Furthermore, hepatic protein levels of Bcl-2, PUMA as well as cCASP3 were all lower in AAV8-*TFAM*/AF mice (Fig. 6G). *TFAM* overexpression did not affect the serum ethanol levels and hepatic protein levels of ADH and CYP2E1 (Supplementary Fig.12C).

ATF4 negatively regulates TFAM expression by suppressing NRF1 in the hepatocyte.

To explore the possible mechanism by which ATF4 negatively regulates TFAM, the effects of alcohol and *ATF4* deletion on major signaling molecules related to mitochondrial biogenesis were measured. As shown in Fig. 7A, the mRNA levels of nuclear respiratory factor 1 (*NRF1*) and peroxisome proliferator-activated receptor gamma coactivator 1-alpha (*PGC-1α)* but not *NRF2* and *PGC-1β* were increased in $ATF4^{\Delta Hep}$/PF mice compared with Flox/PF mice. However, lack of ATF4 in the hepatocytes completely reversed alcohol-decreased expression of *NRF1* but not *PGC-1α*, suggesting that ATF4 may suppress TFAM expression through inhibiting *NRF1* (Fig. 7A). Western blot analysis showed that alcohol-reduced hepatic NRF1 protein levels were reversed by *ATF4* deletion (Fig. 7B). Furthermore, we found that *ATF4* knockdown enhanced the expression of NRF1 in VL-17A cells (Fig. 7C). By contrast, *ATF4* overexpression decreased the mRNA and protein levels of NRF1 (Fig. 7C).

ATF4 positively or negatively regulates the transcription of its target genes via cAMP response element (CRE) sequences [23]. To further determine if ATF4 represses *NRF1* transcription, a series of human *NRF1* promoter constructs with (P3 and P4) or without (P1 and P2) CRE-binding sites were created and co-transfected into 293T cells with *ATF4* overexpression CRISPR plasmids. As shown in Fig. 7D, overexpression of *ATF4* significantly inhibited P3 and P4 promoter activity in reporter assays. However, no activity was observed when promoters P1 and P2 were used (Fig. 7D). Our bioinformatics analysis further identified conserved elements at the ATF4 binding site in the human and mouse *NRF1* promoters (Supplementary Fig. 13A, B). When this cAMP response element was mutated or deleted in promoter P3, trans-inhibition of promoter activity by *ATF4* was absent (Fig. 7E).

We next found that *NRF1* overexpression significantly increased the mRNA and protein levels of TFAM in VL-17 cells, but *NRF1* knockdown decreased the expression of TFAM (Fig. 7F). The cellular mtDNA levels were altered correlatively following TFAM expressions (Fig. 7F). Furthermore, *ATF4* overexpression-decreased TFAM expression, mtDNA contents, and mtDNA-encoded complexes subunits expression were markedly reversed by *NRF1* overexpression (Fig. 7G and Supplementary Fig. 13C). By contrast, *ATF4* knockdown-increased TFAM expression, mtDNA levels, and *MTCO1* expression were all abrogated by *NRF1* knockdown (Fig. 7G). Alcohol-induced mitochondrial membrane potential disruption, OXPHOS dysfunction, and mitochondrial apoptotic pathway activation were ameliorated by *NRF1* overexpression in VL-17A cells (Supplementary Fig. 14A–C).

The NRF1-TFAM signaling pathway is disrupted in the liver of patients with AH.

Finally, we examined the relevance of the identified ATF4-NRF1-TFAM pathway in patients with AH. In contrast to robust induction of ATF4, as described above, remarkable decreases in hepatic mRNA (Fig. 8A) and protein (Fig. 8B) levels of NRF1 and TFAM were observed in AH patients compared with healthy subjects. IHC staining further confirmed significant decreases in nuclear NRF1 and cytoplasmic TFAM as well as MTCO1 proteins in the liver of AH patients (Fig. 8C). The hepatic mtDNA contents and the protein levels of mtDNA-encoded complexes subunits were all significantly decreased in the liver of AH patients (Fig. 8D and E). Nuclear-encoded proteins involved in OXPHOS were also decreased in AH patients (Supplementary Fig. 15A). Decreased hepatic complex I activity (Fig. 8F) was observed in the livers of AH patients. Meanwhile, AH patients exhibited higher levels of hepatic oxidative damage than healthy controls, as indicated by elevated 4-HNE protein adducts formation in the liver (Supplementary Fig. 15B). The protein levels of hepatic PUMA and cleaved caspase-3 were also higher in AH patients than that in healthy subjects (Supplementary Fig. 15C). Collectively, these data indicate that ATF4-mediated NRF1-TFAM signaling pathway disruption may be involved in AH patients.

Discussion

The present study demonstrated, for the first time, that ATF4 plays a critical role in the development of ALD by transmitting the cellular stress from ER to mitochondria. We observed that the PERK-eIF2α-ATF4 ER stress signaling pathway is activated in

the livers of patients with severe AH. Using hepatocyte-specific *ATF4* knockout mice and *ATF4* deficiency VL-17A cell lines, we identified that hepatocyte ATF4 serves as a critical mediator in alcohol-impaired mitochondrial biogenesis and respiratory functions. Investigations of the underlying mechanisms revealed that hepatic TFAM inhibition, resulting from transcriptional suppression of *NRF1*, is mechanistically involved in ATF4-mediated mitochondrial dysfunction in the pathogenesis of ALD. The protective effects of hepatic *ATF4* deletion and *TFAM* overexpression in alcohol-mediated mitochondrial dysfunction were linked to the amelioration of liver injury, which was evidenced by decreased hepatic steatosis, inflammatory response, and apoptosis (Fig. 8G).

Previous study have reported that hepatic knockout of *ATF4* in mice alleviates alcoholic steatosis by inhibiting the expression of lipogenic genes [16], including fatty acid synthase (FAS) and Acetyl-CoA carboxylase (ACC). In this study, we confirmed the detrimental role of hepatic ATF4 in alcoholic steatosis. Our results also revealed that lack of ATF4 in the liver protects alcohol-induced oxidative stress, immune cells infiltration, and apoptosis. However, we found that the expression levels of FAS and ACC were significantly decreased after chronic ethanol feeding and not affected by *ATF4* deletion (Supplementary Fig. 2D). One possible explanation for these discrepancies is that the different feeding method employed. In comparison with 4 weeks ethanol feeding model used by Li et al., our 8 weeks modified NIAAA model generates more damage to the liver and is therefore more clinically relevant. Indeed, the protein levels of hepatic FAS and ACC were also dramatically decreased in AH patients (Supplementary Fig. 2D).

Previous studies have reported that CHOP, a downstream target of ATF4, is activated after alcohol feeding and is involved in ER stress-induced cell death and mitochondrial dysfunction [24, 25]. Unexpectedly, hepatic abrogation of *ATF4* did not affect CHOP protein levels in the liver regardless of alcohol exposure. Furthermore, the mRNA levels of hepatic Bcl-2-like protein 11 (Bim) and Death receptor 5 (DR5), two transcriptional downstream targets of CHOP [26, 27], were also not affected by *ATF4* ablation (Supplementary Fig. 4C). These results suggested that AFT4 is dispensable for CHOP induction during alcohol-induced ER stress. In addition, lack of ATF4 in intestinal epithelial cells even leads to CHOP induction in ileum and colon [28]. It is noteworthy that a growing number of studies demonstrated that the ATF6 branch of the UPR is also a critical determinant of CHOP dynamics during ER stress [29–31]. Thus, further investigation is required to clarify the mechanisms of CHOP induction after ATF4 deletion in ALD.

TFAM is one of the most abundant mitochondria-localized DNA-binding proteins that control mtDNA replication, transcription, and packaging [32–34]. Whole-body *TFAM* deletion is embryonically lethal due to severe mtDNA deletion in mice [35], and tissue-specific lack of *TFAM* disrupts OXPHOS in different cell populations and generates a variety of alterations that recapitulate phenotypes of mitochondrial diseases in human and mice [6, 36–38]. In this study, we found that ATF4 is a negative regulator of TFAM in hepatocyte. Our results demonstrated that ATF4-mediated disruption of the TFAM-mtDNA signaling axis is a pathological factor for alcohol-injury mitochondrial dysfunction and liver injury. This notion is supported by several findings. Firstly, hepatic *ATF4* ablation enhanced TFAM expression *in vitro* and *in vivo*. Lack of *ATF4* protected against alcohol-

decreased TFAM expression and mtDNA contents in hepatocyte. Conversely, forced *ATF4* overexpressing in hepatocyte is sufficient leads to TFAM suppression and mtDNA content reduction. Secondly, the lack of *TFAM* abrogated the protective effects of *ATF4* ablation on alcohol-induced mitochondrial dysfunction and cell death. Thirdly, hepatocyte-specific *TFAM* overexpression prevented alcohol-induced mitochondrial DNA deletion, complex I activity reduction, mitochondrial membrane potential disruption, and OXPHOS dysfunction. Finally, *TFAM* overexpression in hepatocyte markedly ameliorated alcohol-induced steatosis, apoptosis, and inflammatory cell infiltration in the liver. Collectively, these results suggest ATF4-mediated *TFAM* suppression mechanistically links to alcohol-induced mitochondrial dysfunction and liver damage.

NRF1 is a nuclear transcription factor that functions principally as a positive regulator of mitochondrial biogenesis-related genes, including TFAM [39, 40]. Specific and directly binding of NRF1 to TFAM promoter has been demonstrated by chromatin immunoprecipitation. NRF1 silencing produced a 1:1 knockdown of TFAM expression and decreased mtDNA contents [41, 42]. Sharing the same phenotype as TFAM, the genetic ablation of NRF1 also led to embryonically lethal [43]. These findings suggest that NRF1 is the master regulator in TFAM-mediated mtDNA homeostasis. In the present study, we found that both the protein and mRNA levels of NRF1 were remarkably higher in the liver of $ATF4^{\Delta Hep}$ mice than that in ATF4 floxed mice, regardless of alcohol administration. Our cell culture studies showed that ATF4 overexpression decreased NRF1 expression, but ATF4 knockdown enhanced NRF1 expression. We further found that ATF4 directly suppressed NRF1 transcription by binding at the CRE site in the NRF1 promoter. Moreover, *NRF1* overexpression reversed ATF4-mediated TFAM inhibition and mtDNA depletion, suggesting the ATF4-NRF1 interaction and the subsequent TFAM suppression contribute to alcohol-induced mitochondrial dysfunction and liver injury. However, we could not rule out any other pathological factors that might be involved in ATF4-mediated mitochondrial dysfunction in ALD. Previous study reported that 8-week ethanol feeding plus-one binge strongly induced ER stress in the liver, which was associated with increased fat-specific protein 27 (FSP27) expression [44, 45]. Hepatic deletion of FSP27 protects alcohol-induced mitochondrial dysfunction but not ER stress [44]. Interestingly, ATF4 can induce the expression of peroxisome proliferator-activated receptor gamma (PPARγ) [46], a transcription factor known to promote the expression of FSP27α [47]. Therefore, further studies are necessary to test whether hepatic PPARγ-FSP27 axis upregulation is involved in ATF4-mediated mitochondrial dysfunction in ALD.

In summary, the present study uncovered a novel ATF4-NRF1-TFAM signaling pathway in the pathogenesis of alcoholic steatohepatitis. Our data demonstrate that hepatic ATF4 activation mediates alcohol-induced steatohepatitis by impairing mitochondrial biogenesis and respiratory function. Mechanistically, ATF4 negatively regulates TFAM via transcriptionally repressing NRF1 in the hepatocytes. Furthermore, the clinical relevance between ATF4 activation and NRF1-TFAM signaling pathway disruption was validated in the liver tissues from patients with alcoholic hepatitis. Therefore, targeting ATF4 or downstream NRF1-TFAM signals may be potential strategies for the prevention and treatment of alcoholic liver disease.

Supplementary Material

Refer to Web version on PubMed Central for supplementary material.

Acknowledgment:

We thank Dr. Christopher M. Adams at the University of Iowa for kindly providing the *ATF4*-floxed mice, and Dr. Dahn L. Clemens at the University of Nebraska for kindly providing the VL-17A cell line.

Financial support: This research was supported by the National Institutes of Health grants R01AA018844 (Zhanxiang Zhou), R01AA020212 (Zhanxiang Zhou), R24AA025017 (Zhaoli Sun), and Postdoctoral Fellowship Award from American Liver Foundation (Liuyi Hao).

Abbreviation:

ALD	alcoholic liver disease
PERK	protein kinase R (PKR)-like endoplasmic reticulum kinase
AH	alcoholic hepatitis
eIF2α	eukaryotic translation initiation factor 2A
ATF4	activating transcription factor 4
ALT	alanine aminotransferase
AST	aspartate aminotransferase
H&E	hematoxylin and eosin
TUNEL	terminal deoxynucleotidyl transferase dUTP nick end labeling
CHOP	C/EBP homologous protein
PUMA	p53 upregulated modulator of apoptosis
Bcl-2	B-cell lymphoma 2
cCASP3	cleaved caspase-3
NRF1	nuclear respiratory factor 1
TFAM	mitochondrial transcription factor A
OXPHOS	oxidative phosphorylation
ROS	reactive oxygen species
MFI	mean fluorescence intensity
ATP	Adenosine triphosphate
mtDNA	mitochondrial DNA
MTCO1	cytochrome c oxidase subunit 1

MTATP6	mitochondrial encoded ATP synthase membrane subunit 6
SDH	succinate dehydrogenase
TMRE	tetramethylrhodamine, ethyl ester
ADH	alcohol dehydrogenases
CYP2E1	cytochrome P450 2E1
OCR	oxygen consumption rate
NAD	nicotinamide adenine dinucleotide
MTCYB	Cytochrome b
NDUFB8	ubiquinone oxidoreductase subunit B8
ND2	NADH dehydrogenase 2
ND6	NADH dehydrogenase 6
COX5b	Cytochrome c oxidase subunit 5B
Bim	Bcl-2-like protein 11
DR5	death receptor 5
UQCRC2	ubiquinol-cytochrome C reductase core protein 2
MPO	Myeloperoxidase
F4/80	EGF-like module-containing mucin-like hormone receptor-like 1
UPR	unfolded protein response
ACC	acetyl-CoA carboxylase
FAS	fatty acid synthase
FSP27	fat-specific protein 27
PPARγ	peroxisome proliferator-activated receptor gamma
CRE	cAMP response element

Reference

[1]. Gao B, Bataller R. Alcoholic liver disease: pathogenesis and new therapeutic targets. Gastroenterology2011;141:1572–1585. [PubMed: 21920463]

[2]. Seitz HK, Bataller R, Cortez-Pinto H, et al.Alcoholic liver disease. Nature reviews Disease primers2018;4:16.

[3]. Thursz M, Kamath PS, Mathurin P, et al.Alcohol-related liver disease: Areas of consensus, unmet needs and opportunities for further study. Journal of hepatology2019;70:521–530. [PubMed: 30658117]

[4]. Spinelli JB, Haigis MC. The multifaceted contributions of mitochondria to cellular metabolism. Nature cell biology2018;20:745–754. [PubMed: 29950572]

[5]. Koopman WJ, Distelmaier F, Smeitink JA, et al.OXPHOS mutations and neurodegeneration. The EMBO journal2013;32:9–29. [PubMed: 23149385]

[6]. Baixauli F, Acin-Perez R, Villarroya-Beltri C, et al.Mitochondrial Respiration Controls Lysosomal Function during Inflammatory T Cell Responses. Cell metabolism2015;22:485–498. [PubMed: 26299452]

[7]. Wang J, Silva JP, Gustafsson CM, et al.Increased in vivo apoptosis in cells lacking mitochondrial DNA gene expression. Proceedings of the National Academy of Sciences of the United States of America2001;98:4038–4043. [PubMed: 11259653]

[8]. Mansouri A, Gattolliat CH, Asselah T. Mitochondrial Dysfunction and Signaling in Chronic Liver Diseases. Gastroenterology2018;155:629–647. [PubMed: 30012333]

[9]. Fromenty B, Grimbert S, Mansouri A, et al.Hepatic mitochondrial DNA deletion in alcoholics: association with microvesicular steatosis. Gastroenterology1995;108:193–200. [PubMed: 7806041]

[10]. Tang C, Liang X, Liu H, et al.Changes in mitochondrial DNA and its encoded products in alcoholic cirrhosis. International journal of clinical and experimental medicine2012;5:245–250. [PubMed: 22837799]

[11]. Ji CNew Insights into the Pathogenesis of Alcohol-Induced ER Stress and Liver Diseases. International journal of hepatology2014;2014:513787. [PubMed: 24868470]

[12]. Dara L, Ji C, Kaplowitz N. The contribution of endoplasmic reticulum stress to liver diseases. Hepatology2011;53:1752–1763. [PubMed: 21384408]

[13]. Nishitoh HCHOP is a multifunctional transcription factor in the ER stress response. Journal of biochemistry2012;151:217–219. [PubMed: 22210905]

[14]. Xiao Y, Deng Y, Yuan F, et al.An ATF4-ATG5 signaling in hypothalamic POMC neurons regulates obesity. Autophagy2017;13:1088–1089. [PubMed: 28350524]

[15]. Yoshizawa T, Hinoi E, Jung DY, et al.The transcription factor ATF4 regulates glucose metabolism in mice through its expression in osteoblasts. The Journal of clinical investigation2009;119:2807–2817. [PubMed: 19726872]

[16]. Li K, Xiao Y, Yu J, et al.Liver-specific Gene Inactivation of the Transcription Factor ATF4 Alleviates Alcoholic Liver Steatosis in Mice. The Journal of biological chemistry2016;291:18536–18546. [PubMed: 27405764]

[17]. Seo J, Fortuno ES 3rd, Suh JM, et al.Atf4 regulates obesity, glucose homeostasis, and energy expenditure. Diabetes2009;58:2565–2573. [PubMed: 19690063]

[18]. Quiros PM, Prado MA, Zamboni N, et al.Multi-omics analysis identifies ATF4 as a key regulator of the mitochondrial stress response in mammals. The Journal of cell biology2017;216:2027–2045. [PubMed: 28566324]

[19]. Hao L, Sun Q, Zhong W, et al.Mitochondria-targeted ubiquinone (MitoQ) enhances acetaldehyde clearance by reversing alcohol-induced posttranslational modification of aldehyde dehydrogenase 2: A molecular mechanism of protection against alcoholic liver disease. Redox biology2018;14:626–636. [PubMed: 29156373]

[20]. Hori O, Ichinoda F, Tamatani T, et al.Transmission of cell stress from endoplasmic reticulum to mitochondria: enhanced expression of Lon protease. The Journal of cell biology2002;157:1151–1160. [PubMed: 12082077]

[21]. Xie Y, He Y, Cai Z, et al.Tauroursodeoxycholic acid inhibits endoplasmic reticulum stress, blocks mitochondrial permeability transition pore opening, and suppresses reperfusion injury through GSK-3ss in cardiac H9c2 cells. American journal of translational research2016;8:4586–4597. [PubMed: 27904664]

[22]. Chen Q, Thompson J, Hu Y, et al.Metformin attenuates ER stress-induced mitochondrial dysfunction. Translational research : the journal of laboratory and clinical medicine2017;190:40–50. [PubMed: 29040818]

[23]. Koyanagi S, Hamdan AM, Horiguchi M, et al.cAMP-response element (CRE)-mediated transcription by activating transcription factor-4 (ATF4) is essential for circadian expression

of the Period2 gene. The Journal of biological chemistry2011;286:32416–32423. [PubMed: 21768648]

[24]. Zhang W, Zhong W, Sun Q, et al.Adipose-specific lipin1 overexpression in mice protects against alcohol-induced liver injury. Scientific reports2018;8:408. [PubMed: 29323242]

[25]. Chen X, Zhong J, Dong D, et al.Endoplasmic Reticulum Stress-Induced CHOP Inhibits PGC-1alpha and Causes Mitochondrial Dysfunction in Diabetic Embryopathy. Toxicological sciences : an official journal of the Society of Toxicology2017;158:275–285. [PubMed: 28482072]

[26]. Puthalakath H, O'Reilly LA, Gunn P, et al.ER stress triggers apoptosis by activating BH3-only protein Bim. Cell2007;129:1337–1349. [PubMed: 17604722]

[27]. Yamaguchi H, Wang HG. CHOP is involved in endoplasmic reticulum stress-induced apoptosis by enhancing DR5 expression in human carcinoma cells. The Journal of biological chemistry2004;279:45495–45502. [PubMed: 15322075]

[28]. Hu X, Deng J, Yu T, et al.ATF4 Deficiency Promotes Intestinal Inflammation in Mice by Reducing Uptake of Glutamine and Expression of Antimicrobial Peptides. Gastroenterology2019;156:1098–1111. [PubMed: 30452920]

[29]. Fusakio ME, Willy JA, Wang Y, et al.Transcription factor ATF4 directs basal and stress-induced gene expression in the unfolded protein response and cholesterol metabolism in the liver. Molecular biology of the cell2016;27:1536–1551. [PubMed: 26960794]

[30]. Yang H, Niemeijer M, van de Water B, et al.ATF6 Is a Critical Determinant of CHOP Dynamics during the Unfolded Protein Response. iScience2020;23:100860. [PubMed: 32058971]

[31]. Lebeaupin C, Vallee D, Hazari Y, et al.Endoplasmic reticulum stress signalling and the pathogenesis of non-alcoholic fatty liver disease. Journal of hepatology2018;69:927–947. [PubMed: 29940269]

[32]. Kang I, Chu CT, Kaufman BA. The mitochondrial transcription factor TFAM in neurodegeneration: emerging evidence and mechanisms. FEBS letters2018;592:793–811. [PubMed: 29364506]

[33]. Matsushima Y, Goto Y, Kaguni LS. Mitochondrial Lon protease regulates mitochondrial DNA copy number and transcription by selective degradation of mitochondrial transcription factor A (TFAM). Proceedings of the National Academy of Sciences of the United States of America2010;107:18410–18415. [PubMed: 20930118]

[34]. Dolle C, Flones I, Nido GS, et al.Defective mitochondrial DNA homeostasis in the substantia nigra in Parkinson disease. Nature communications2016;7:13548.

[35]. Larsson NG, Wang J, Wilhelmsson H, et al.Mitochondrial transcription factor A is necessary for mtDNA maintenance and embryogenesis in mice. Nature genetics1998;18:231–236. [PubMed: 9500544]

[36]. Vernochet C, Mourier A, Bezy O, et al.Adipose-specific deletion of TFAM increases mitochondrial oxidation and protects mice against obesity and insulin resistance. Cell metabolism2012;16:765–776. [PubMed: 23168219]

[37]. Koh JH, Johnson ML, Dasari S, et al.TFAM Enhances Fat Oxidation and Attenuates High-Fat Diet-Induced Insulin Resistance in Skeletal Muscle. Diabetes2019;68:1552–1564. [PubMed: 31088855]

[38]. Li H, Wang J, Wilhelmsson H, et al.Genetic modification of survival in tissue-specific knockout mice with mitochondrial cardiomyopathy. Proceedings of the National Academy of Sciences of the United States of America2000;97:3467–3472. [PubMed: 10737799]

[39]. Kiyama T, Chen CK, Wang SW, et al.Essential roles of mitochondrial biogenesis regulator Nrf1 in retinal development and homeostasis. Molecular neurodegeneration2018;13:56. [PubMed: 30333037]

[40]. Jornayvaz FR, Shulman GI. Regulation of mitochondrial biogenesis. Essays in biochemistry2010;47:69–84. [PubMed: 20533901]

[41]. Piantadosi CA, Suliman HB. Mitochondrial transcription factor A induction by redox activation of nuclear respiratory factor 1. The Journal of biological chemistry2006;281:324–333. [PubMed: 16230352]

[42]. Gao W, Wu M, Wang N, et al.Increased expression of mitochondrial transcription factor A and nuclear respiratory factor-1 predicts a poor clinical outcome of breast cancer. Oncology letters2018;15:1449–1458. [PubMed: 29434836]

[43]. Huo L, Scarpulla RC. Mitochondrial DNA instability and peri-implantation lethality associated with targeted disruption of nuclear respiratory factor 1 in mice. Molecular and cellular biology2001;21:644–654. [PubMed: 11134350]

[44]. Xu MJ, Cai Y, Wang H, et al.Fat-Specific Protein 27/CIDEC Promotes Development of Alcoholic Steatohepatitis in Mice and Humans. Gastroenterology2015;149:1030–1041 e1036. [PubMed: 26099526]

[45]. Liangpunsakul S, Gao B. Alcohol and fat promote steatohepatitis: a critical role for fat-specific protein 27/CIDEC. Journal of investigative medicine : the official publication of the American Federation for Clinical Research2016;64:1078–1081. [PubMed: 27342423]

[46]. Yu K, Mo D, Wu M, et al.Activating transcription factor 4 regulates adipocyte differentiation via altering the coordinate expression of CCATT/enhancer binding protein beta and peroxisome proliferator-activated receptor gamma. The FEBS journal2014;281:2399–2409. [PubMed: 24673832]

[47]. Matsusue K, Kusakabe T, Noguchi T, et al.Hepatic steatosis in leptin-deficient mice is promoted by the PPARgamma target gene Fsp27. Cell metabolism2008;7:302–311. [PubMed: 18396136]

Significance of this study

What is already known on this subject?

- Hepatic *ATF4* is activated by chronic alcohol exposure in mice and liver-specific *ATF4* deletion protects alcoholic steatosis.
- Mitochondrial dysfunction contributes to alcohol-induced liver injury in mice.

What are the new findings?

- Hepatocyte-specific ablation of *ATF4* protects alcohol-induced mitochondrial dysfunction in mouse liver.
- ATF4 acts as a negative regulator of the NRF1-TFAM signaling pathway *in vivo* and *in vitro*.
- Overexpressing *TFAM* in hepatocyte protects against alcohol-induced mitochondrial dysfunction and steatohepatitis in mice.
- The clinical relevance between ATF4 activation and NRF1-TFAM signaling pathway disruption is validated in the liver tissues from patients with severe alcoholic hepatitis.

How might it impact on clinical practice in the foreseeable future?

These findings suggest that expression of ATF4 in hepatocytes plays a critical role in the development of alcoholic liver disease. Targeting ATF4 and downstream NRF1-TFAM signals may be potential strategies for the prevention and treatment of alcoholic liver disease.

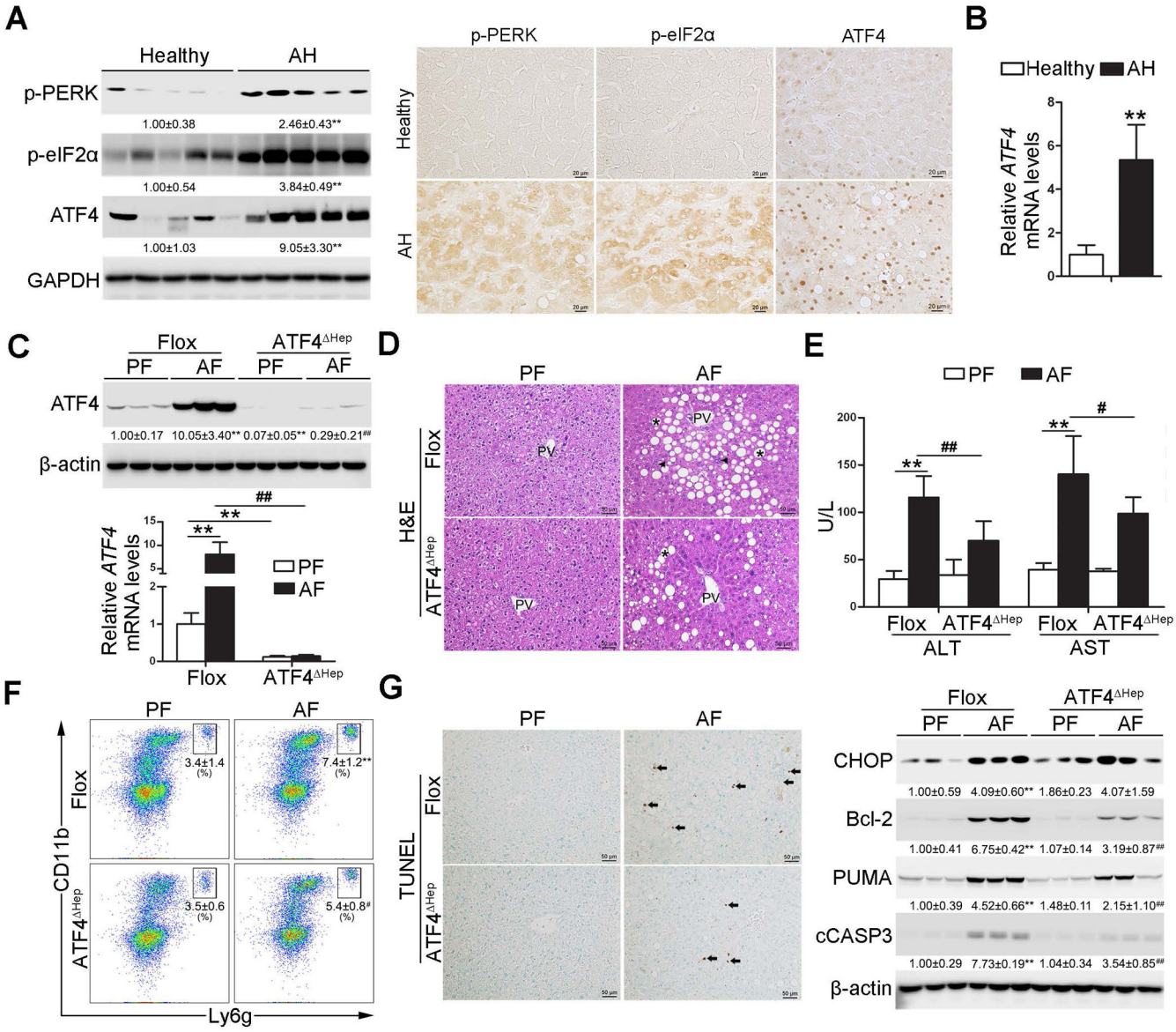

Fig. 1. Hepatic PERK-eIF2α-ATF4 signaling pathway is upregulated in ALD patients and hepatocyte-specific ablation of *ATF4* protects alcohol-induced liver injury in mice.

(A-B) Liver tissues were obtained from ALD patients and healthy controls. (A) Western bolt and immunohistochemistry analysis of hepatic PERK-eIF2α-ATF4 signaling expression (n=5/group). Scale bars: 20 μm. (B) Analysis of mRNA levels of *ATF4* in the livers (n=5/group). (C-G) ATF4 floxed and ATF4$^{\Delta Hep}$ male mice were pair-fed or alcohol-fed for 8 weeks plus a single binge of ethanol (4 g/kg) before 4 hours of tissue collection. (C) Protein and mRNA levels of ATF4 in the liver (n=3–8). (D) Liver histopathological changes shown by H&E staining. Scale bars: 50 μm. Asterisks: lipid droplets. Arrowheads: Infiltrated immune cells. (E) Serum ALT and AST activities (n=8–11). (F) Representative dot plot and gating strategy for 7-AAD^{-}CD45^{+}CD11b^{+} Ly6g^{+} neutrophils (n=6). (G) Immunohistochemistry of TUNEL and Western bolt analysis of hepatic CHOP, Bcl-2, PUMA, and cleaved caspase-3. Scale bars: 50 μm. Arrow: TUNEL positive cells. Protein

bands intensity was quantified by ImageJ (NIH). Data are presented as means ± SD. In panels A and B, statistical comparisons were made using Student's *t*-test; **P<0.01 vs. healthy control. In panels C-G, statistical comparisons were made using one-way ANOVA with Tukey's post hoc test; **P<0.01 vs. Flox/PF mice; #P<0.05, ##P<0.01 vs. Flox/AF mice. PF, pair-fed; AF, alcohol-fed.

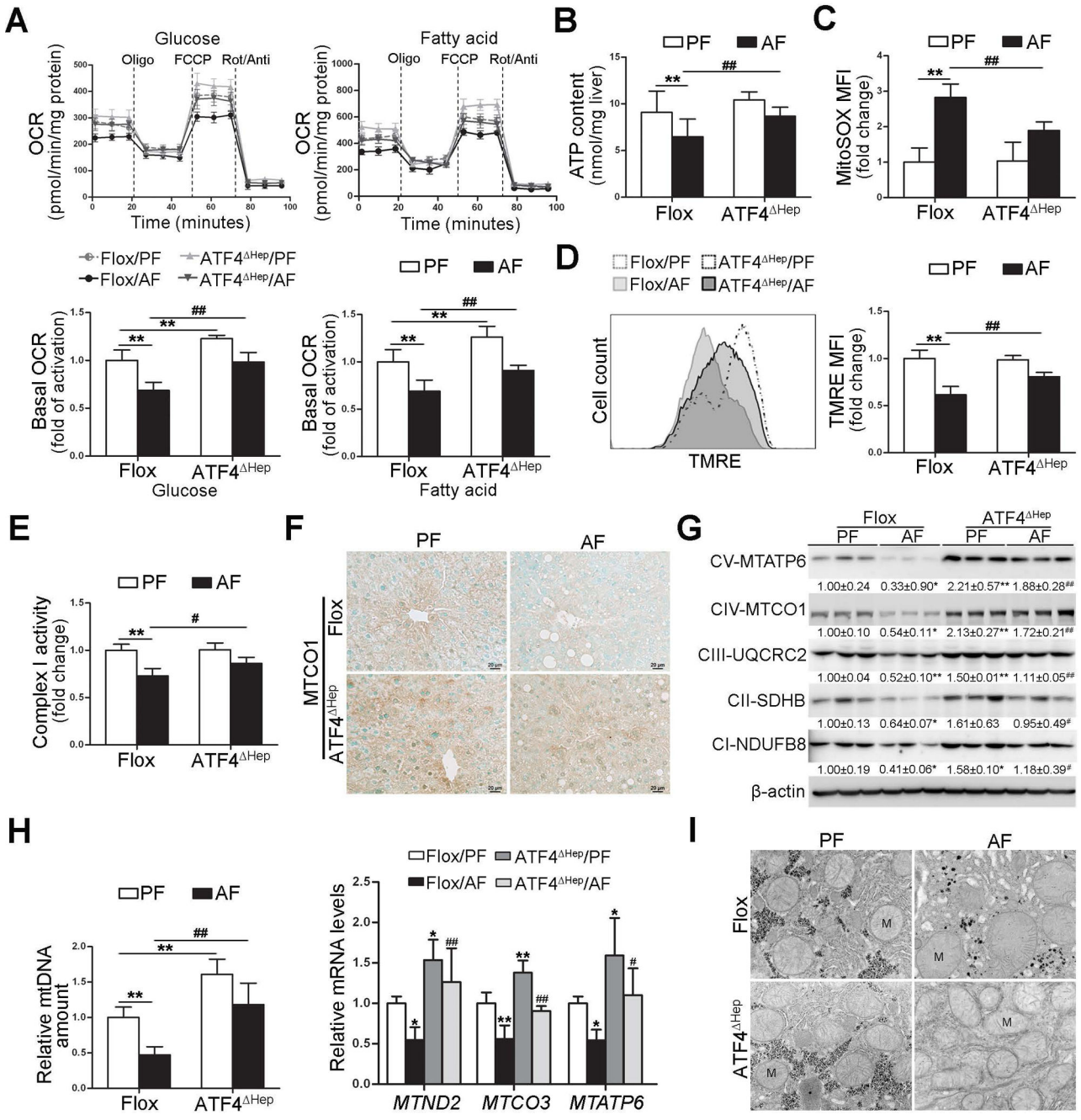

Fig. 2. Ablation of *ATF4* in hepatocyte protects alcohol-mediated mitochondrial dysfunction in the liver.

ATF4 floxed and ATF4$^{\Delta Hep}$ male mice were pair-fed or alcohol-fed for 8 weeks plus a single binge (4 g/kg) before 4 hours of tissue collection. (A) Representative oxygen consumption rate profile (OCR) and basal OCR in isolated primary hepatocytes. (B) ATP contents in the liver (n=5). (C) FACS analysis of mitochondrial ROS using MitoSOX dye (n=5). Data are the summary of the mean fluorescence intensity (MFI). (D) FACS analysis of mitochondrial membrane potential using TMRE probe (n=5). Data are the summary of the mean fluorescence intensity (MFI). (E) Hepatic complex I activity

(n=6). (F) Immunohistochemistry of MTCO1 in the liver. Images were captured by light microscope. Scale bars: 20 μm. (G) Western blot analysis of mitochondrial respiratory complexes subunits (MTATP6, MTCO1, UQCRC2, SDHB, and NDUFB8). (H) mtDNA levels (MTND1) relative to nuclear DNA (SDHA) and the mRNA levels of mtDNA-encoded complexes subunits (n=5–6). (I) Mitochondrial morphology and ultrastructure. Protein bands intensity was quantified by ImageJ (NIH). Data are presented as means ± SD. Statistical comparisons were made using one-way ANOVA with Tukey's post hoc test. *P<0.05, **P<0.01 vs. Flox/PF mice; #P<0.05, ##P<0.01 vs. Flox/AF mice. PF, pair-fed; AF, alcohol-fed; M, mitochondria.

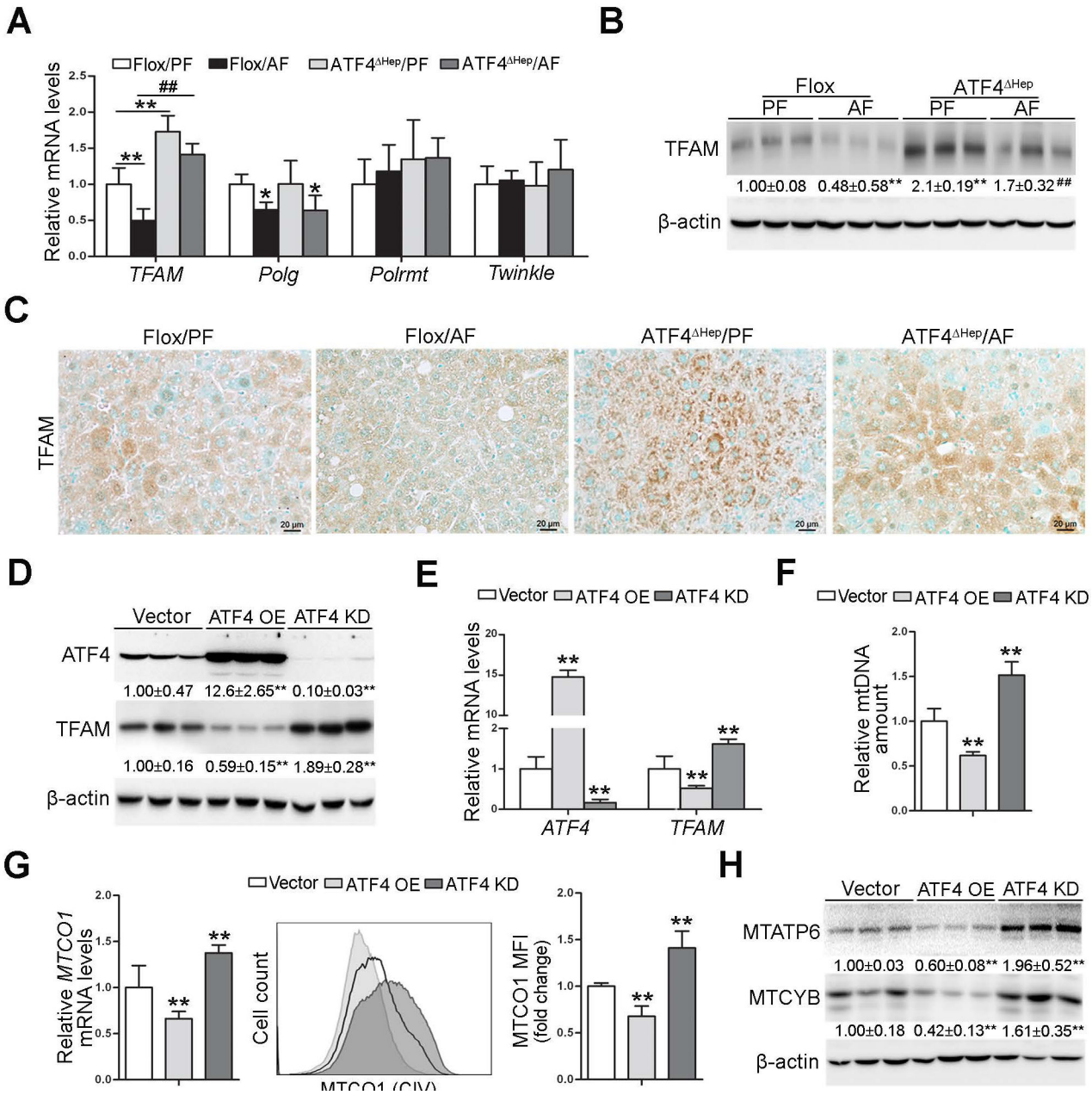

Fig. 3. ATF4 negatively regulates TFAM in hepatocyte.

(A-C) ATF4 floxed and ATF4$^{\Delta Hep}$ male mice were pair-fed or alcohol-fed for 8 weeks plus a single binge of ethanol (4 g/kg) 4 hours before tissue collection. (A) Relative mRNA levels of hepatic *TFAM*, *Polg*, *Polrmt*, and *Twinkle* (n=5). (B) Western blot of hepatic TFAM. (C) Immunohistochemistry of hepatic TFAM. Images were captured by light microscope. Scale bars: 20 μm. (D-H) VL-17 cells were transfected with either *ATF4* overexpression or *ATF4* knockdown CRISPR plasmids. (D) Western blot analysis of ATF4 and TFAM in VL-17A cells. (E) Analysis of mRNA levels of *ATF4* and *TFAM* in VL-17A cells (n=5–8). (F) mtDNA levels (MTND1) relative to nuclear DNA (SDHA) in VL-17A cells (n=6). (G) The mRNA levels and protein levels of MTCO1 were measured by RT-PCR and flow cytometry,

respectively (n=4–6). (H) Western blot analysis of MTATP6 and MTCYB in VL-17A cells. Protein bands intensity was quantified by ImageJ (NIH). Data are presented as means ± SD. Statistical comparisons were made using one-way ANOVA with Tukey's post hoc test. Panel A and B, *P<0.05, **P<0.01 vs. Flox/PF mice. ##P<0.01 vs. Flox/AF mice. Panel D-H, **P<0.01 vs. control cells. PF, pair-fed; AF, alcohol-fed.

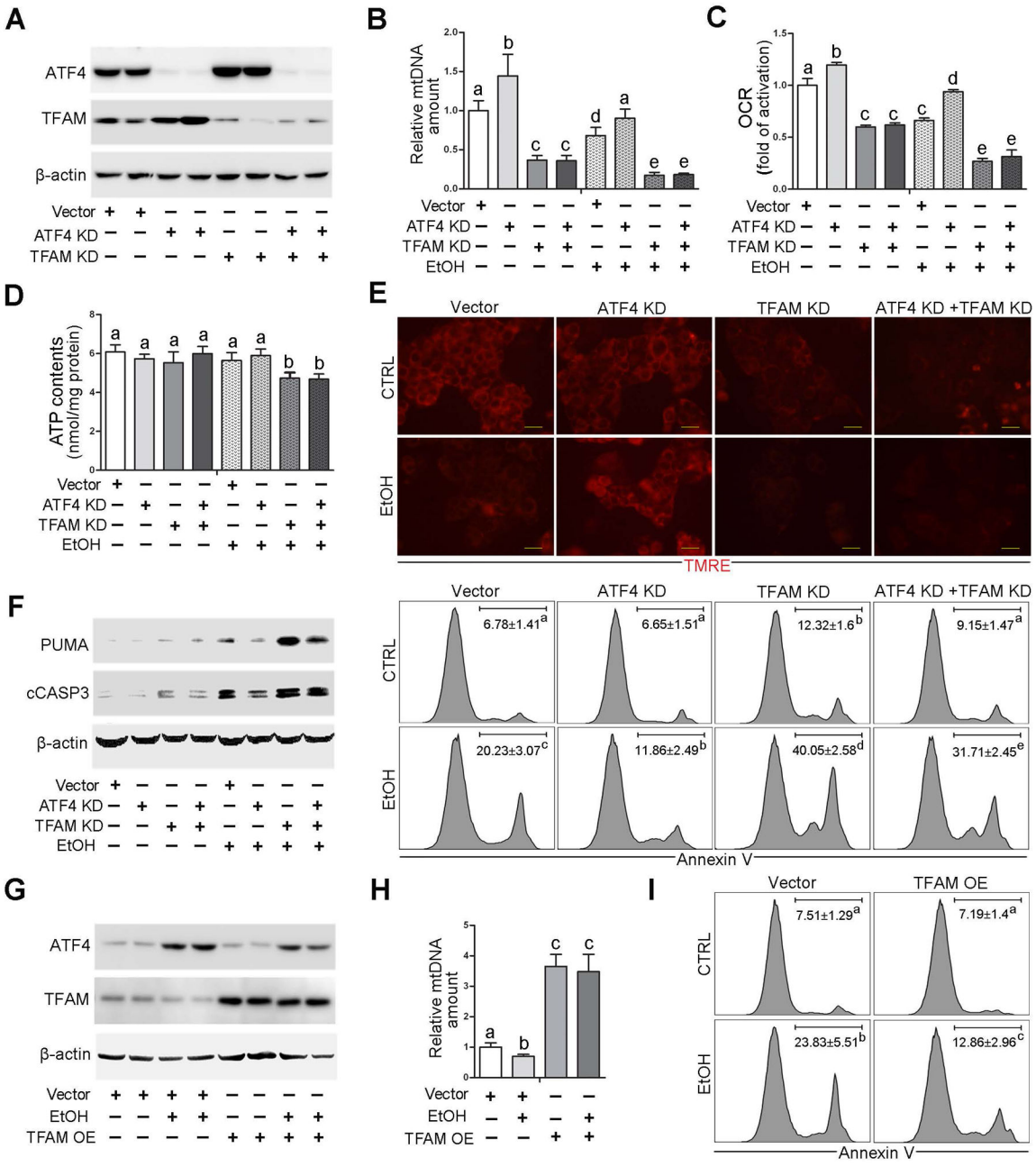

Fig. 4. TFAM reduction is involved in ATF4-mediated mitochondrial dysfunction in VL-17A cells with alcohol exposure.

ATF4 knockdown, *TFAM* knockdown, *ATF4/TFAM* double knockdown VL-17A cells were generated and treated with 100 mM ethanol for 72 hours. (A) Western blot analysis of ATF4 and TFAM. (B) mtDNA levels (*MTND1*) relative to nuclear DNA (*SDHA*) in VL-17A cells (n=5). (C) Basal oxygen consumption rate of VL-17A cells (n=6). (D) ATP contents in VL-17A cells (n=5). (E) Immunofluorescent staining of mitochondrial membrane potential using TMRE probe. Scale bars: 20 μm. (F) Western blot analysis of PUMA and cleaved caspase-3, and FACS analysis of apoptotic cell death represented by Annexin V positive cells (n=4–6). (G-I) VL-17 cells were transfected with *TFAM* overexpression CRISPR

plasmids and treated with 100 mM ethanol for 72 hours. (G) Western blot analysis of ATF4 and TFAM in VL-17A cells. (H) mtDNA levels (*MTND1*) relative to nuclear DNA (*SDHA*) in *TFAM* overexpression cells (n=5). (I) FACS analysis of apoptotic cell death represented by Annexin V positive cells. Protein bands intensity was quantified by ImageJ (NIH). Data are presented as means ± SD. Statistical comparisons were made using one-way ANOVA with Tukey's post hoc test. Bars with different characters differ significantly ($P < 0.05$). EtOH, ethyl alcohol.

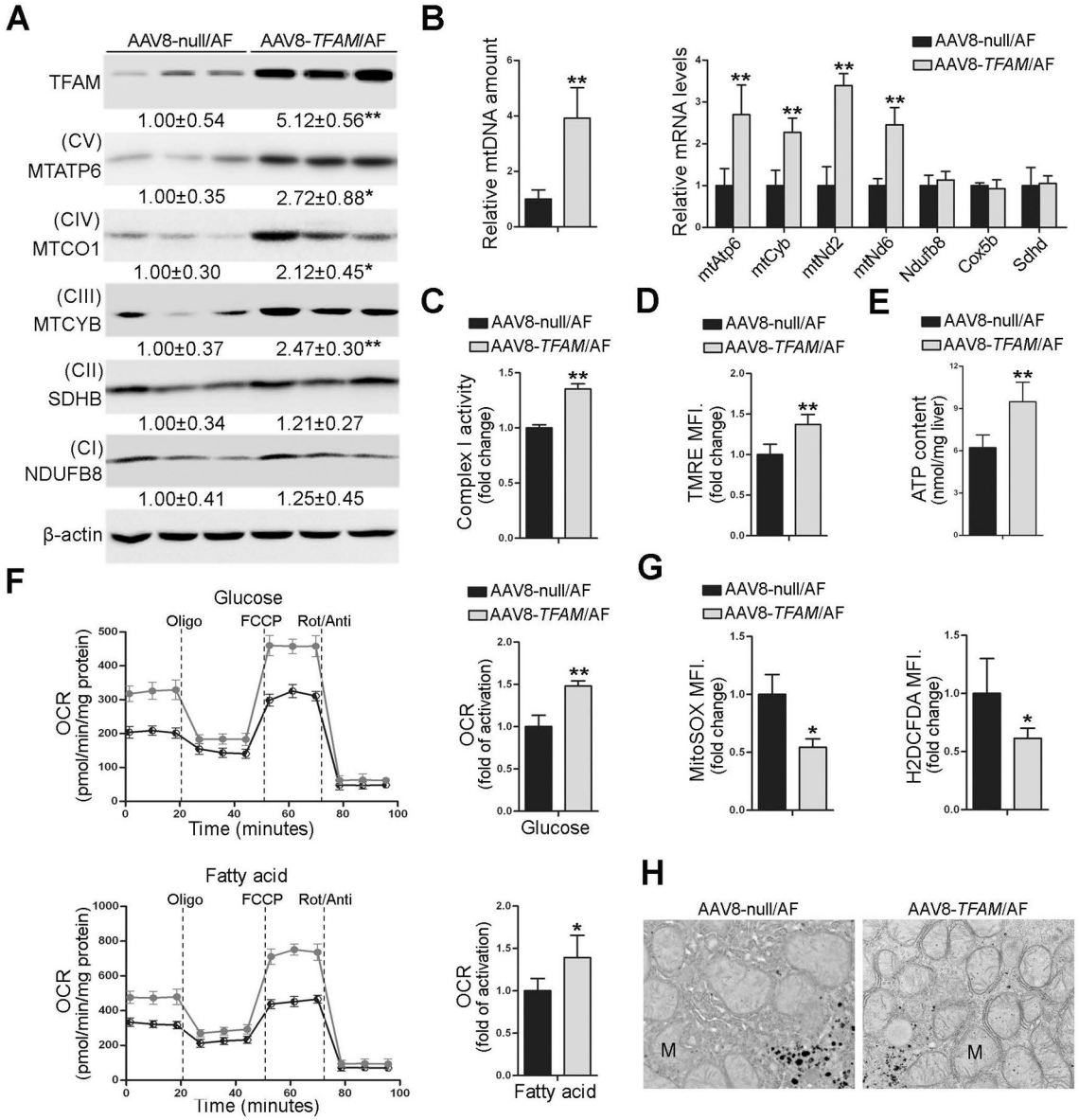

Fig. 5. Hepatocyte-specific *TFAM* overexpression protects alcohol-induced mitochondrial dysfunction in mice.

Hepatocyte-specific *TFAM* overexpression mice were generated by injected in the retrial orbital sinus with recombinant adeno-associated viral (AAV) serotype 8 gene transfer vectors bearing a liver-specific promoter combination (TBG) with mouse *TFAM* sequence. Mice injected with null-vector are served as control. These mice were fed with alcohol for 8 weeks plus a single binge of alcohol (4 g/kg) 4 hours before tissue collection. (A) Protein levels of TFAM, MTATP6, MTCO1, MTCYB, SDHB, and NDFUB8 in the liver. (B) Hepatic mtDNA contents (*MTND1* relative to *SDHA*) and mtDNA- and nuDNA-encoded genes expression (n=4–6). (C) Hepatic mitochondrial complex I activity (n=5). (D) FACS analysis of mitochondrial membrane potential using TMRE probe (n=5). Data are the summary of the mean fluorescence intensity (MFI). (E) ATP contents in the liver (n=5). (F) Representative oxygen consumption rate profile (OCR) and basal OCR in isolated primary

hepatocytes. (G) FACS analysis of mitochondrial ROS and total ROS using MitoSOX dye and H2DCFDA dye, respectively (n=5). Data are the summary of the mean fluorescence intensity (MFI). (H) Mitochondrial morphology and ultrastructure. Protein bands intensity was quantified by ImageJ (NIH). Data are presented as means ± SD. Statistical comparisons were made using one Student's *t*-test. *P<0.05, **P<0.01 vs. AAV8-null/AF mice. AF, alcohol-fed; M, mitochondria.

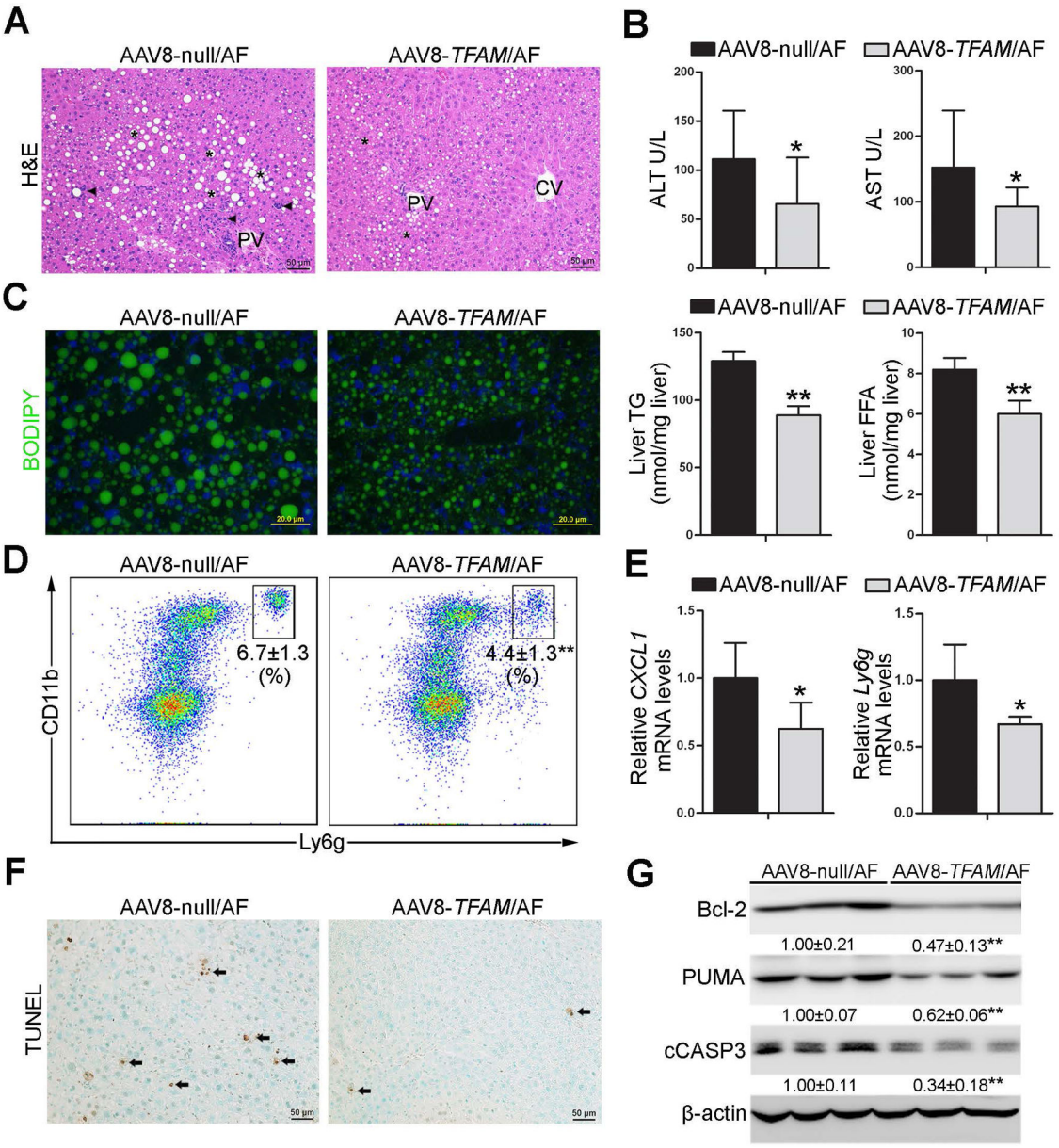

Fig. 6. Hepatocyte-specific *TFAM* overexpression ameliorates alcoholic steatohepatitis in mice.

Hepatocyte-specific *TFAM* overexpression mice were generated by injected in the retrial orbital sinus with recombinant adeno-associated viral (AAV) serotype 8 gene transfer vectors bearing a liver-specific promoter combination (TBG) with mouse *TFAM* sequence. Mice injected with null-vector are served as control. These mice were fed with alcohol for 8 weeks plus a single binge of alcohol (4 g/kg) 4 hours before tissue collection. (A) H&E staining. Scale bars: 50 μm. Asterisks: lipid droplets. Arrowheads: Infiltrated immune cells. (B) Serum ALT and AST activities (n=6). (C) BODIPY staining of the neutral lipids in mouse liver, and hepatic TG and FFA contents (n=6). Scale bars: 20 μm. (D) Representative dot plot for $CD11b^+$ and $Ly6g^+$ neutrophils are displayed of singlet $7\text{-}AAD^-$ $CD45^+$ cells (n=5). (E) The mRNA levels of hepatic *Cxcl-1* and *Ly6g* (n=5). (F) Immunohistochemistry of hepatic TUNEL. Scale bars: 50 μm. Arrow: TUNEL positive cells. (G) The protein levels

of Bcl-2, PUMA, and cleaved caspase3 in the liver. Protein bands intensity was quantified by ImageJ (NIH). Data are presented as means ± SD. Statistical comparisons were made using one Student's *t*-test. *P<0.05, **P<0.01 vs. AAV8-null/AF mice. AF, alcohol-fed.

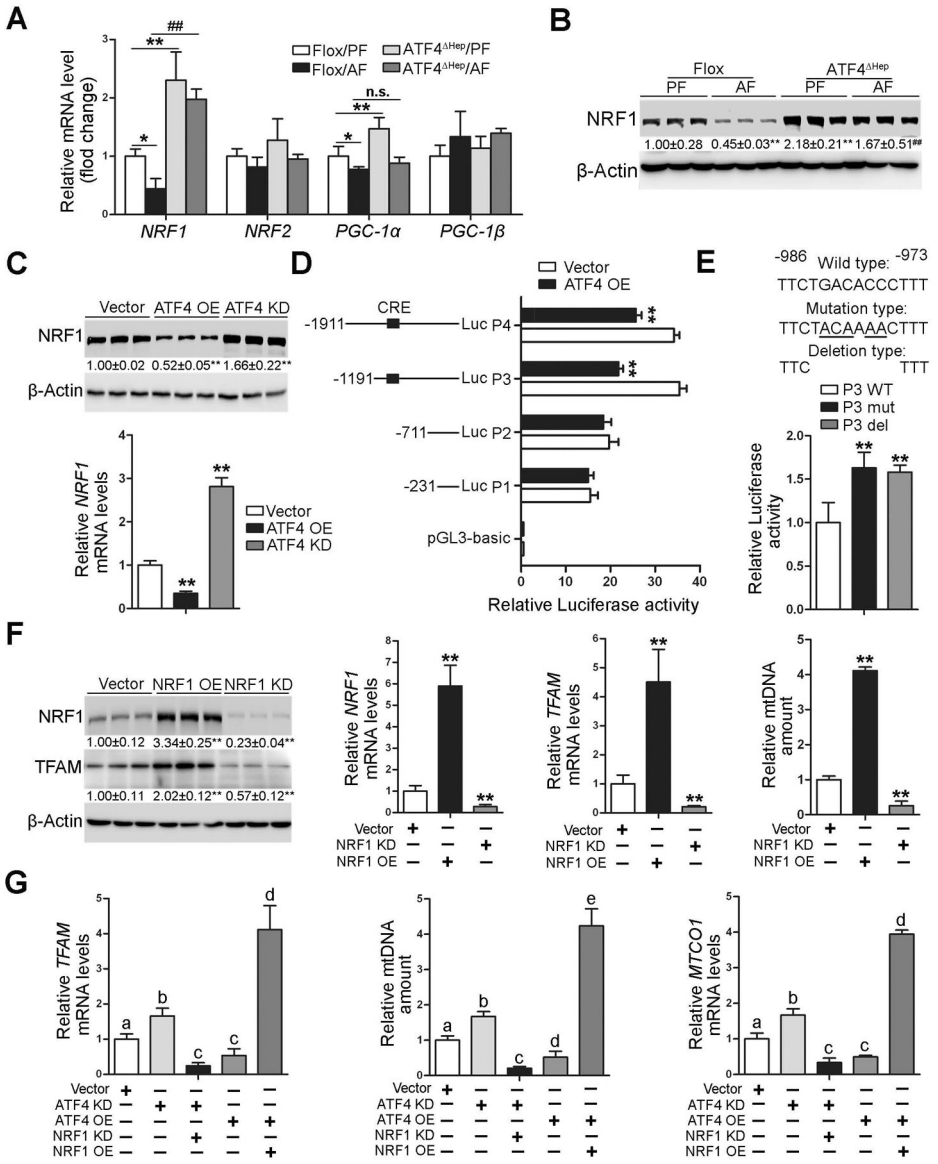

Fig. 7. NRF1 is directly interact and inactivated by ATF4.

(A-B) ATF4 floxed and ATF4$^{\Delta Hep}$ male mice were pair-fed or alcohol-fed for 8 weeks plus a single binge of ethanol (4 g/kg) 4 hours before tissue collection. (A) Analysis of mRNA levels of *NRF1*, *NRF2*, *PGC-1α*, and *PGC-1β* in livers (n=5). (B) Western blot analysis of NRF1. (C) The expression of NRF1 in VL-17A cells transfected with either *ATF4* overexpression CRISPR plasmid or *ATF4* knockdown CRISPR plasmid. (D) The Relative luciferase activity of *NRF1* promoters. (E) Relative promoter activity of wild-type of P3 (P3 WT) promoter and the mutated (P3 mut) and deleted (P3 del) constructs. The dual-luciferase activity was measured after 48 h transfection. (F) The protein levels and mRNA levels of NRF1 and TFAM after transfected either *NRF1* overexpression CRISPR plasmid or *NRF1* knockdown CRISPR plasmid. (G) Relative *TFAM* mRNA levels, mtDNA contents (*MTND1* relative to *SDHA*), and mRNA levels of *MTCO1* in *ATF4/NRF1* double overexpression and *ATF4/NRF1* double knockout VL-17A cell lines. Protein bands intensity

was quantified by ImageJ (NIH). Data are presented as means ± SD. Statistical comparisons were made using one-way ANOVA with Tukey's post hoc test (n=3–6). In panels A and B, *P<0.05, **P<0.01 vs. Flox/PF mice; # P<0.05, ##P<0.01 vs. Flox/AF mice. In panels C-F, **P < 0.05 versus corresponding control. In panel G, bars with different characters differ significantly (P < 0.05). PF, pair-fed; AF, alcohol-fed.

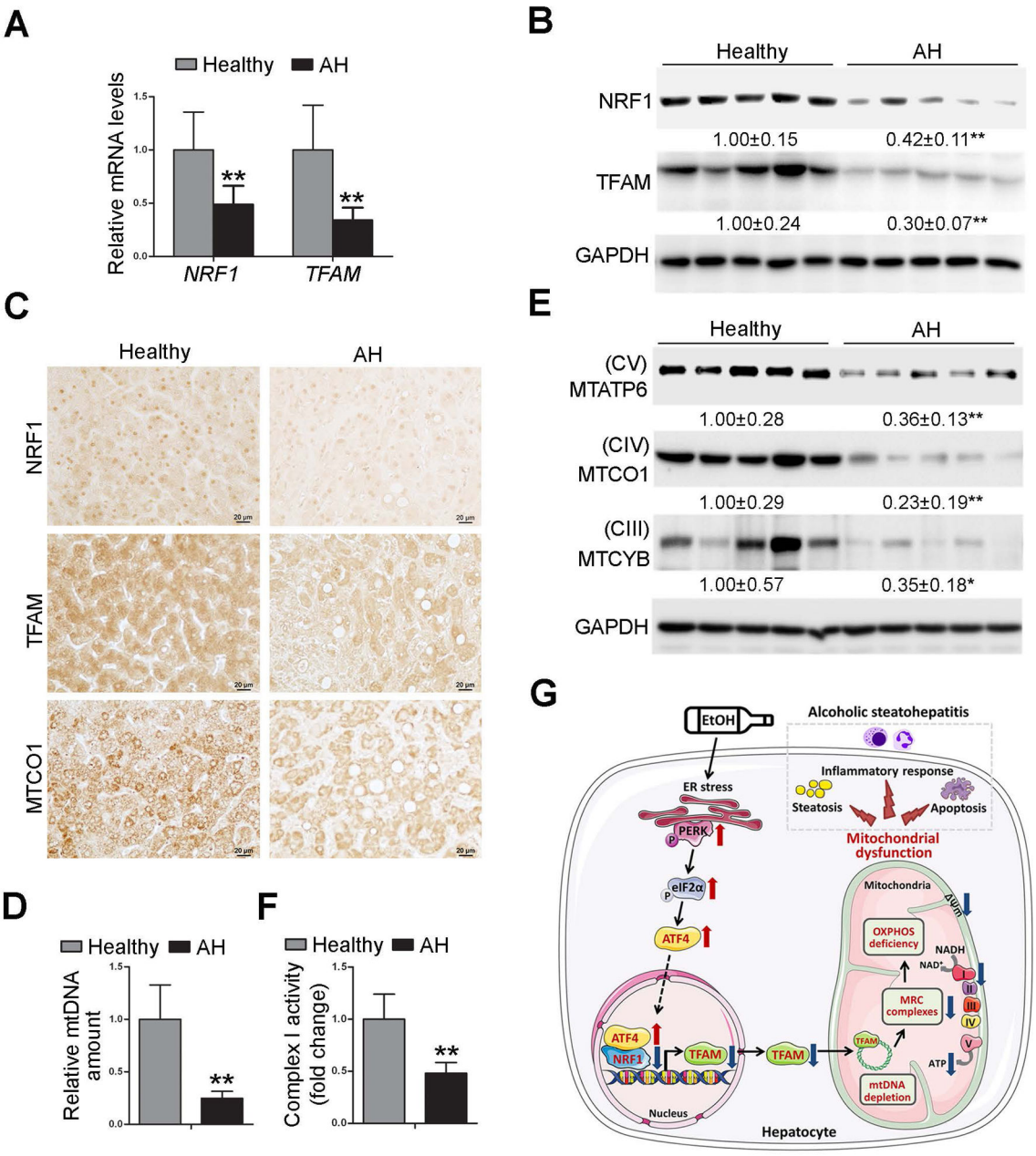

Fig. 8. NRF1-TFAM signaling pathway is disrupted in the liver of patients with alcoholic hepatitis.

We obtained liver tissues from severe ALD patients and healthy donors. (A) The mRNA levels of hepatic *NRF1* and *TFAM* (n=5). (B) Western blot analysis of hepatic NRF1 and TFAM. (C) Immunohistochemistry staining of NRF1, TFAM, and MTCO1 in the liver. Images were captured by light microscope. Scale bars: 20 μm. (D) mtDNA levels (MTND1) relative to nuclear DNA (SDHA) in the liver (n=5). (E) Western blot analysis of hepatic MTATP6, MTCO1, and MTCYB (n=5). (F) Hepatic complex I activity (n=5). Protein bands intensity was quantified by ImageJ (NIH). Data are presented as means ±

SD. Statistical comparisons were made using Student's *t*-test (n=5). *P<0.05, **P<0.01 vs. healthy controls.